



Semi-supervised adversarial deep learning for capacity estimation of battery energy storage systems

Jiachi Yao^a, Zhonghao Chang^{b,c}, Te Han^{b,c,*}, Jingpeng Tian^{d,**}

^a School of Mechanical-Electronic and Vehicle Engineering, Beijing University of Civil Engineering and Architecture, Beijing, 100044, China

^b Center for Energy and Environmental Policy Research, Beijing Institute of Technology, Beijing, 100081, China

^c School of Management, Beijing Institute of Technology, Beijing, 100081, China

^d Department of Electrical and Electronic Engineering and Research Centre for Grid Modernization, The Hong Kong Polytechnic University, Kowloon, Hong Kong, 999077, China



ARTICLE INFO

Handling Editor: Prof X Ou

Keywords:

Lithium-ion batteries

Battery ageing

Capacity estimation

Semi-supervised learning

Adversarial learning

ABSTRACT

Battery energy storage systems (BESS) play a pivotal role in energy management, and the precise estimation of battery capacity is crucial for optimizing their performance and ensuring reliable power supply. Deep learning methodologies applied to battery capacity estimation have exhibited exemplary performance. However, deep learning methods necessitate supervised training with a significant volume of labeled data, presenting challenges for data collection in industrial scenarios. Moreover, a diverse range of battery types in industrial settings makes it difficult to develop capacity estimation models for different types of batteries from scratch. To address these issues, a semi-supervised adversarial deep learning (SADL) method is proposed for lithium-ion battery capacity estimation. Initially, a subset of labeled lithium-ion battery data, coupled with a subset of unlabeled data, is collected. Voltage and current data are then transformed into capacity increment features. Subsequently, an adversarial training strategy is employed, subjecting labeled and unlabeled data to adversarial training to enhance the performance of SADL. Finally, the effectiveness of the SADL method in estimating the capacity of other lithium-ion batteries is analysed. Experimental results demonstrate that the SADL method accurately estimates the capacity of various battery types, showcasing an RMSE error of approximately 2%, surpassing the performance of other methods. The proposed SADL method emerges as a promising solution for the precise estimation of lithium-ion battery capacity in BESS.

1. Introduction

Battery Energy Storage Systems (BESS) are integral to modern energy management and grid applications due to their prowess in storing and releasing electrical energy. Their significance lies in enhancing grid stability by balancing demand and supply, seamlessly integrating renewable energy sources, and providing crucial backup power during peak demand or grid disruptions. BESS plays a vital role in fortifying the reliability, efficiency, and sustainability of power systems, playing a key part in the transition toward a more robust and renewable energy future. In BESS, lithium-ion batteries emerge as the mainstream technology. Since John B. Goodenough invented the lithium iron phosphate cathode material, lithium-ion batteries have significantly impacted the world. In comparison to lead-acid and nickel-metal hydride batteries, lithium-ion

batteries offer distinct advantages, including high self-discharge efficiency, exceptional energy density, long cycle life, absence of pollution, and no memory effect [1,2]. For instance, lithium-ion batteries boast a minimum of 800–10,000 charge/discharge cycles, self-discharge efficiency below 8% per month, and a weight-specific energy ranging from 150 to 300 Wh/kg.

Lithium-ion batteries, acting as the predominant and representative technology in BESS, find extensive applications in diverse scenarios, including grid energy storage, renewable energy storage, electric vehicles, factory emergency power systems, and electronic devices. In these application scenarios, the crucial roles of battery management systems and battery capacity estimation are progressively gaining prominence [3,4]. In terms of safety prevention, monitoring the battery state is instrumental in the early identification of aging issues, effectively

* Corresponding author. Center for Energy and Environmental Policy Research, Beijing Institute of Technology, Beijing, 100081, China.

** Corresponding author.

E-mail addresses: hante@bit.edu.cn (T. Han), jinpeng.tian@polyu.edu.hk (J. Tian).

reducing safety risks, and providing robust support for battery maintenance [5,6]. In optimizing battery charging/discharging and implementing cycling utilization, accurate estimation of battery capacity can achieve precise control of battery charging/discharging process [7]. This assists in formulating rational strategies for battery management, enhancing energy utilization efficiency, and reducing energy wastage. Additionally, the state of health of batteries is crucial for retirement and subsequent utilization [8]. Through battery management systems and capacity estimation, the suitability of batteries for continued use can be determined. This is vital for formulating scientifically strategies for battery decommissioning and reuse, contributing to environmental conservation, and maximizing the value of batteries. In general, battery management systems and battery capacity estimation play critical roles in safety precautions, battery maintenance, strategy formulation, and charging optimization. They are essential for improving battery reliability, extending lifespan, and reducing maintenance costs.

However, as lithium-ion batteries age with time and charge-discharge cycles, they undergo significant changes. Lithium-ion batteries undergo chemical reactions during charge and discharge cycles, forming solid electrolyte interface layers on electrodes [9]. The accumulation of solid electrolyte interface layers increases internal resistance, reducing conductivity and causing capacity fade. Additionally, the repeated expansion and contraction of electrode materials induce mechanical stress, leading to structural changes like particle cracking and electrode pulverization. These factors compromise battery integrity and contribute to capacity degradation over time. Notably, battery aging raises the risk of temperature elevation, potentially causing overheating and short circuits, thereby increasing safety concerns [10]. The capacity of lithium-ion batteries is a direct and crucial indicator of their performance and condition. Accurate capacity estimation is essential for efficient industrial battery management, ensuring economic benefits, and mitigating safety risks associated with performance degradation in lithium-ion batteries [11].

Currently, researchers have proposed numerous methods for estimating the capacity of lithium-ion batteries, broadly categorized into model-based and data-driven methods [12,13]. In model-based approaches, the fundamental concept involves developing a lithium-ion battery model based on electrochemical processes and physical parameters, with subsequent capacity estimation based on the constructed model. The commonly employed model is the equivalent circuit model (ECM) [14]. Krishnan S. Hariharan developed a nonlinear ECM to analyse the state of lithium-ion batteries [15]. The traditional ECM has a limited number of resistor-capacitor (RC) networks. To improve accuracy, Farnmann et al. utilized high-order RC networks [16]. Yang et al. proposed an improved ECM based on parallel-connected RC networks, building upon the traditional ECM [17]. However, the increased complexity resulting from high-order RC networks poses challenges such as heightened computational burden and model stability issues [18]. To address these concerns and maintain precision in lithium-ion battery modeling, researchers explored model reduction methods [19,20]. As the array of ECMS continues to expand, researchers have conducted comparative analyses to evaluate their performance. Hu et al. conducted a comparative analysis of twelve ECMS for lithium-ion batteries [21], while Peng et al. compared and analysed the influence of different ECM parameters [22]. Another widely used model is the electrochemical model. Since Doyle's introduction of the lithium-ion electrochemical model in the last century, this model has evolved due to its capacity to reflect electrochemical processes within batteries [23,24]. Electrochemical models can be constructed from both a physical structure and mathematical formula perspective. Physical structure-based models include pseudo-two-dimensional model [25], three-dimensional model [26], single particle model [27,28], etc. Constructing electrochemical models through mathematical formulas primarily involves developing partial differential equations using finite difference and finite element techniques [29,30].

The model-based methods, rooted in a deep understanding of

electrochemical processes and physical parameters, demonstrate exceptional accuracy in simulating capacity degradation trends for specific lithium-ion batteries. These approaches offer valuable insights into the underlying electrochemical mechanisms, enhancing our comprehension of battery behavior [31,32]. Nevertheless, their primary limitation lies in the difficulty of directly applying constructed models to different lithium-ion battery types due to the absence of certain physics and confidential parameters [33]. The challenges associated with obtaining essential parameters for the diverse array of lithium-ion batteries further hinder the generalizability of model-based methods, making them less suitable for widespread application.

In contrast, the primary advantage of data-driven methods lies in their ability to analyse the state of lithium-ion batteries solely through data, without the need to consider the complex physicochemical structure within the batteries. However, their drawback is the dependence on data, and the interpretability is relatively weak. Data-driven methods can be further categorized into machine learning and deep learning methods [34]. Numerous researchers have explored machine learning-based capacity estimation techniques for lithium-ion batteries. For instance, Wu et al. proposed a PCA-PSO-BPNN method for estimating the state of health in lithium-ion batteries, demonstrating its efficacy in NASA battery tests [35]. Sun et al. combined SVM with a discrete battery aging model to enhance the accuracy of capacity estimation for lithium-ion batteries [36]. Compared to shallow network structures like BPNN and SVM, deep learning models excel in feature extraction. Consequently, researchers have delved into deep learning-based methods for lithium-ion battery capacity estimation, employing techniques such as CNN [37–39], LSTM [40–42], DBN [43], graph neural networks [44], among others.

Despite the rapid advancements in deep learning for lithium-ion battery capacity estimation, training deep learning models heavily rely on abundant battery voltage and current data, along with their corresponding capacity data, for supervised training. For most battery data, acquiring voltage and current data is relatively straightforward, but obtaining accurate corresponding capacity data poses a challenge. Obtaining capacity data necessitates complete charge-discharge cycles for the battery. Due to incomplete charge and discharge processes, the capacity data cannot be acquired, leading to the inability to utilize labeled data for training deep learning models. There are two main reasons for the existence of unlabeled capacity data in battery datasets. Firstly, acquiring capacity data necessitates extensive and complete charge-discharge testing experiments on batteries at various degradation states, consuming a substantial amount of time and electrical energy. For instance, the NASA lithium-ion battery degradation data involved several hundred charge-discharge experiments, making it a costly endeavor. Secondly, in battery application scenarios such as electric vehicles and grid energy storage, there is an abundance of voltage and current data without corresponding capacity labels [45]. This is because most batteries do not undergo complete charge-discharge cycles in practical usage. Typically, charging begins when the battery still has a significant amount of remaining capacity. Due to the lack of complete charge-discharge cycles, it is not possible to obtain accurate capacity data. In the case of a significant amount of unlabeled data within the battery dataset, it is essential to fully consider these unlabeled data to develop a deep learning method that can accurately estimate the capacity of lithium-ion batteries. This is crucial for aiding in the maintenance and management of batteries.

In order to fully leverage unlabeled battery data, researchers have proposed semi-supervised lithium-ion battery capacity estimation methods. For instance, Xiong et al. proposed a semi-supervised CNN method for estimating battery capacity [46]. Salucci et al. also proposed a semi-supervised learning method, demonstrating relatively low errors in estimating the state of lithium-ion batteries [47]. Semi-supervised deep learning methods demonstrate accurate lithium-ion battery capacity estimation. However, the diverse battery types in real industrial scenarios pose a challenge. Directly applying a trained model to

different batteries may result in suboptimal capacity estimation accuracy. To address this issue, researchers have explored transfer learning techniques to enhance accuracy in lithium-ion battery capacity estimation [48–51]. While transfer learning methods effectively improve accuracy, they necessitate a small amount of battery data for model fine-tuning. Acquiring such labeled data in real industrial scenarios is challenging due to the varied battery types, leading to increased costs and potential concerns related to data security and privacy.

In response to these challenges, this work proposes a novel semi-supervised deep learning approach. The proposed method maximizes the utilization of existing unlabeled data and enhances model performance through adversarial learning strategies, thereby achieving accurate estimation of diverse battery capacities in industrial settings. The primary contributions of this work include:

- (1) The proposed semi-supervised deep learning approach capitalizes on the wealth of unlabeled battery data available in industrial settings, supplemented by a limited amount of labeled data. This method is specifically designed to tackle the intricate task of lithium-ion battery capacity estimation within industrial scenarios.
- (2) To augment the precision of lithium-ion battery capacity estimation, the proposed method incorporates an adversarial training strategy. This entails subjecting both labeled and unlabeled battery data to adversarial training, facilitating a profound exploration of data features and thereby enhancing the model's accuracy in estimating battery capacity.
- (3) Experimental results affirm the efficacy of the proposed semi-supervised method in accurately estimating lithium-ion battery capacity. The capacity error of batteries estimated by the SADL method remains about 2% margin of the measured capacity. Consequently, the SADL method emerges as a promising approach for battery capacity estimation in industrial contexts.

The following contents are as follows. Section 2 introduces the background and preliminaries. Section 3 presents the proposed semi-supervised method. Section 4 introduces the experimental results and comparative analysis. Finally, the conclusions are presented in section 5.

2. Background and preliminaries

2.1. Challenges for data-driven capacity estimation of lithium-ion batteries

For supervised lithium-ion battery capacity estimation, the lithium-ion battery dataset is $\{(x_i, y_i)\}_{i=1}^N$, where x_i is the feature vector of the i -th battery, and y_i is the corresponding capacity value. The feature vector x_i encompasses measurable signals, such as current, voltage, etc., during the charging/discharging process. Formally, $x_i = [x_{i1}, x_{i2}, \dots, x_{ip}]$, where p represents the number of features. The objective is to establish a deep learning model f by learning a mapping relationship. This model can accurately estimate the capacity value y_n for a new battery feature vector x_n . The deep learning model can be represented as follows.

$$y_i = f(x_i; \theta) + \epsilon_i \quad (1)$$

where f is the deep learning model, θ is the model parameters, and ϵ_i is the error term.

Typically, we choose an appropriate deep learning architecture, such as a multi-layer perceptron (MLP) or convolutional neural network (CNN), and adjust the model parameters θ by training on the dataset D to minimize the estimation error on the training set. This can be achieved by minimizing the loss function L , i.e.,

$$\min_{\theta} \sum_{i=1}^N L(y_i, f(x_i; \theta)) \quad (2)$$

where the loss function L can take different forms, such as mean squared error:

$$L(y_i, f(x_i; \theta)) = (y_i - f(x_i; \theta))^2 \quad (3)$$

However, as mentioned earlier, utilizing only labeled samples can induce considerable effort and costs. Semi-supervised learning is therefore proposed to take advantage of an unlabeled data set to train the deep learning model. In the context of semi-supervised capacity estimation, the dataset is $E = \{(x_i, y_i)\}_{i=1}^N \cup \{(x_j)\}_{j=1}^M$, comprising both labeled and unlabeled samples. Here, N and M denote the numbers of labeled and unlabeled samples, respectively. Each labeled sample x_i consists of the feature vector of battery, with y_i being the corresponding known capacity value. Unlabeled samples x_j solely include the feature vectors. The semi-supervised framework extends the conventional supervised learning paradigm by integrating insights derived from unlabeled samples. The loss function L is augmented to simultaneously consider both kinds of samples.

$$\min_{\theta} \sum_{i=1}^N L(y_i, f(x_i; \theta)) + \lambda \sum_{j=1}^M L(f(x_j; \theta)) \quad (4)$$

where λ serves as a hyperparameter balancing the significance of labeled and unlabeled samples. The loss function L can adopt various forms, such as mean squared error, as mentioned earlier.

2.2. Convolutional neural network

Convolutional Neural Network (CNN) has demonstrated effectiveness in extracting relevant information from lithium-ion battery data [37–39]. A standard CNN architecture consists of fundamental elements, namely convolutional layers, pooling layers, and fully connected layers. The sequential arrangement of convolutional and pooling layers within a CNN facilitates the gradual extraction of progressively abstract features, thereby augmenting the capability of model for estimating the capacity of lithium-ion batteries.

The primary function of the convolutional layer is to extract local features from the data through convolution operations, capturing spatial structures and patterns. The convolution operation is a core component of CNN, involving the sliding of a convolution kernel over input data. The mathematical formulation for one-dimensional convolution is given by:

$$(f * g)[n] = \sum_{m=-\infty}^{\infty} f[m] \cdot g[n-m] \cdot W[m] \quad (5)$$

where f represents the input data, g is the convolution kernel, and W denotes the weights.

The pooling layer plays a pivotal role in dimensionality reduction within CNN, aiming to refine and condense the information derived from preceding convolutional layers. This reduction in feature map size serves multiple purposes, foremost among them being the alleviation of computational complexity and the mitigation of overfitting, a common concern in model training. Pooling operations within this layer act as strategic filters, effectively summarizing the most salient information while discarding redundant or less essential details. Two widely employed pooling techniques are max pooling and average pooling. The operation of max pooling is mathematically expressed as follows.

$$(\mathbf{P}_{\max})(i, j) = \max_{(m, n) \in \Omega} (\mathbf{X})(i+m, j+n) \quad (6)$$

where \mathbf{P}_{\max} represents the output of the max pooling operation, \mathbf{X} is the input, and Ω denotes the pooling region.

The fully connected layer amalgamates features from convolutional and pooling layers, creating a high-level abstraction. Each neuron in the fully connected layer connects to all neurons in the previous layer, with

connections having weights W_{ij} . The *ReLU* activation function is applied as follows.

$$FC = \text{ReLU} \left(\sum_{j=1}^N W_{ij} x_j + b_i \right) \quad (7)$$

2.3. Adversarial training

In 2014, Ian Goodfellow pioneered the generative adversarial network (GAN) model [52]. Since the proposal of GAN, it has emerged rapidly and become one of the most eye-catching deep learning models. GAN is specifically designed to fortify the model against minor perturbations in the input data by introducing adversarial samples. The GAN model consists of generators and discriminators trained through adversarial learning, dynamically seeking an optimal solution in a homomorphic equilibrium. The underlying concept of GAN is rooted in game theory, leveraging the adversarial interplay between the generator and discriminator to enhance model performance. The generator is responsible for producing data, while the discriminator performs binary classification, determining whether the data is a generated sample or a real sample. Throughout training, the performance of both generators and discriminators continually improves through dynamic adversarial training. The flow diagram of GAN model is illustrated in Fig. 1.

GAN model is a combination of the characteristics of generative model and discriminant model. Through the way of dynamic confrontation training, this antagonistic process gives GAN a significant advantage. The objective function of GAN is as follows.

$$\min_G \max_D V(D, G) = \mathbb{E}_{x \sim p_{\text{data}}(x)} [\log D(x)] + \mathbb{E}_{z \sim p_z(z)} [\log (1 - D(G(z)))] \quad (8)$$

where $\mathbb{E}_{x \sim p_{\text{data}}(x)} [\log D(x)]$ means to sample the actual data distribution and then find the expectation of the function $\log D(x)$. $\mathbb{E}_{z \sim p_z(z)} [\log (1 - D(G(z)))]$ means to sample from Gaussian noise and find the expectation of the function $\log (1 - D(G(z)))$.

The adversarial training process of the generator and discriminator is as follows. During the discriminator parameter update phase, the generator's parameters remain static, forming the foundational stage of adversarial training. The central aim is the meticulous adjustment of the discriminator's parameters to refine its discriminatory prowess. This adjustment process is integral to optimizing the discriminator's ability to distinguish between real and generated samples. The objective function is as follows.

$$\max_D V(D, G) = \mathbb{E}_{x \sim p_{\text{data}}(x)} [\log D(x)] + \mathbb{E}_{z \sim p_z(z)} [\log (1 - D(G(z)))] \quad (9)$$

where $\mathbb{E}_{x \sim p_{\text{data}}(x)} [\log D(x)]$ scrutinizes the discriminator's classification of real samples. $\mathbb{E}_{z \sim p_z(z)} [\log (1 - D(G(z)))]$ assesses its classification of generated samples.

Subsequently, in the generator parameter update phase, the discriminator's parameters are treated as constants, allowing focused attention on fine-tuning the generator's parameters. The primary goal is to strategically influence the data generation process, rendering generated samples more challenging for the discriminator to classify. This fine-tuning endeavor is designed to heighten the realism of the

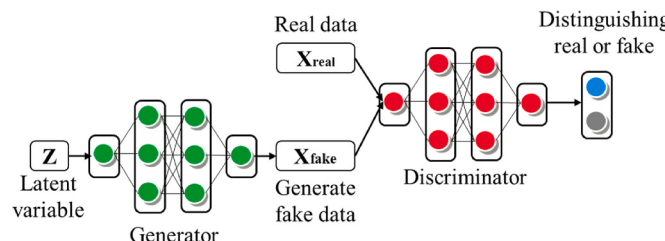


Fig. 1. The structure of GAN.

generated data. The objective function is as follows.

$$\min_G V(D, G) = \mathbb{E}_{x \sim p_{\text{data}}(x)} [\log D(x)] + \mathbb{E}_{z \sim p_z(z)} [\log (1 - D(G(z)))] \quad (10)$$

where $\mathbb{E}_{x \sim p_{\text{data}}(x)} [\log D(x)]$ evaluates the discriminator's classification of real samples. $\mathbb{E}_{z \sim p_z(z)} [\log (1 - D(G(z)))]$ scrutinizes its classification of generated samples

Through the intricate interplay of these optimization phases, the model progressively converges to a dynamic equilibrium. This equilibrium manifests as a generator capable of producing highly realistic data and a discriminator endowed with heightened discriminatory acumen. The adversarial training methodology embedded in this iterative optimization process empowers the GAN to not only generate high-quality authentic data but also maintain robustness and resilience in the face of adversarial challenges.

3. Proposed method

3.1. Input and output for capacity estimation model of batteries

In industrial settings, lithium-ion battery voltage and current data are measured. However, as an input for analysis, the incremental capacity (IC) curves, derived from the voltage and current, is utilized. This is because the capacity increment feature is more effective in capturing the dynamic state evolution of lithium-ion batteries compared to voltage and current data, as indicated by previous research [40,50]. The capacity increment feature, denoted as dQ/dV , is calculated using the formula $I \times dt/dV$.

In this work, the training dataset for training the SADL model consists of labeled battery data $D_l = \{(x_i, y_i)\}_{i=1}^N$ and unlabeled battery data $D_u = \{(x_j)\}_{j=1}^M$. After training the SADL model, the testing dataset $T = \{(x_k, y_k)\}_{k=1}^Q$ is utilized to assess its performance. The y_k denotes the actual capacity of the battery test set. The objective is to minimize the error between the estimated capacity \hat{y}_k by the SADL model and the actual capacity y_k .

3.2. Semi-supervised adversarial deep learning

Deep learning demonstrates remarkable capabilities in feature extraction, and GANs significantly boost model performance through adversarial training. To refine the accuracy of lithium-ion battery capacity estimation, a semi-supervised adversarial deep learning (SADL) approach is proposed. The SADL method not only capitalizes on the convolutional feature extraction proficiency but also enhances the model's efficacy through the integration of an adversarial training strategy.

In addressing the lithium-ion battery capacity estimation challenge in this study, it is unnecessary to employ a generator for generating spurious samples to adversarially contend with real samples. The lithium-ion battery training dataset comprises labeled battery data $D_l = \{(x_i, y_i)\}_{i=1}^N$ and unlabeled battery data $D_u = \{(x_j)\}_{j=1}^M$. CNN is employed to extract features from dataset. Subsequently, an adversarial training strategy is applied to facilitate adversarial learning of the extracted features from D_l and D_u . In essence, CNN is employed to discern common features across D_l and D_u , enabling the resulting model's applicability to other batteries.

In the SADL method, the convolutional feature extraction module $G_f(\cdot; \theta_f)$ is employed to extract features from the D_l and D_u data. The discrimination module $G_d(\cdot; \theta_d)$ is then utilized to discern whether the data originates from the D_l (labeled) or D_u (unlabeled) dataset. The objective is to ensure that the discrimination module $G_d(\cdot; \theta_d)$ cannot differentiate whether the data comes from the labeled D_l or unlabeled D_u dataset. In the context of binary cross-entropy (BCE), the output loss function for an input sample x_i is expressed as follows.

$$\mathcal{L}_d(G_d(G_f(x_i)), d_i) = -d_i \log(G_d(G_f(x_i)) - (1-d_i)\log(1-G_d(G_f(x_i))) \quad (11)$$

For labeled battery data sets $D_l = \{(x_i, y_i)\}_{i=1}^N$ and unlabeled battery data sets $D_u = \{(x_j)\}_{j=1}^M$, there is the following formula.

$$E(\theta_f, \theta_d) = -\left(\frac{1}{N}\sum_{i=1}^N \mathcal{L}_d^i(\theta_f, \theta_d) + \frac{1}{M}\sum_{i=1}^M \mathcal{L}_d^i(\theta_f, \theta_d)\right) \quad (12)$$

where $\mathcal{L}_d^i(\theta_f, \theta_d) = \mathcal{L}_d(G_d(G_f(x_i; \theta_f); \theta_d), d_i)$.

The discrimination module $G_d(\cdot; \theta_d)$ and feature extraction module $G_f(\cdot; \theta_f)$ are trained alternately by the following two formulas to form an antagonistic mechanism.

$$\hat{\theta}_d = \operatorname{argmax}_{\theta_d} E(\hat{\theta}_f, \theta_d) \quad (13)$$

$$\hat{\theta}_f = \operatorname{argmin}_{\theta_f} E(\theta_f, \hat{\theta}_d) \quad (14)$$

By optimizing $\hat{\theta}_d$, $G_d(\cdot; \theta_d)$ can more accurately distinguish feature attributes. By optimization $\hat{\theta}_f$, making $G_d(\cdot; \theta_d)$ difficult to judge feature field attributes. The feature extraction ability of the model can be improved by alternate training.

For the lithium-ion battery capacity estimation problem, assuming the data is $\{(x_i, y_i)\}_{i=1}^N$, the mean square error (MSE) loss function can be expressed as follows.

$$\mathcal{L}_y(G_y(G_f(x_i; \theta_f); \theta_y), y_i) = \frac{1}{N} \sum_{i=1}^N (y_i - G_y(x_i; \theta_y))^2 \quad (15)$$

where $G_y(\cdot; \theta_y)$ is the capacity estimation module.

In this regard, the model optimization objective function can be expressed as follows.

$$E(\theta_f, \theta_y) = \frac{1}{N} \sum_{i=1}^N \mathcal{L}_y^i(\theta_f, \theta_y) - \lambda \Phi(\theta_f, \theta_y) \quad (16)$$

where $\mathcal{L}_y^i(\theta_f, \theta_y) = \mathcal{L}_y(G_y(G_f(x_i; \theta_f); \theta_y), y_i)$. λ is the hyperparameter. Φ is the regular term.

Considering the above optimization problems, the following formula can be obtained.

$$E(\theta_f, \theta_y, \theta_d) = \frac{1}{N} \sum_{i=1}^N \mathcal{L}_y^i(\theta_f, \theta_y) - \lambda \left(\frac{1}{N} \sum_{i=1}^N \mathcal{L}_d^i(\theta_f, \theta_d) + \frac{1}{M} \sum_{i=1}^M \mathcal{L}_d^i(\theta_f, \theta_d) \right) - \lambda \Phi(\theta_f, \theta_y) \quad (17)$$

The parameter update strategy is as follows.

$$\theta_f \leftarrow \theta_f - \mu \left(\frac{\partial \mathcal{L}_y^i}{\partial \theta_f} + \lambda \frac{\partial \mathcal{L}_d^i}{\partial \theta_f} \right) \quad (18)$$

$$\theta_d \leftarrow \theta_d - \mu \frac{\partial \mathcal{L}_d^i}{\partial \theta_d} \quad (19)$$

$$\theta_y \leftarrow \theta_y - \mu \frac{\partial \mathcal{L}_y^i}{\partial \theta_y} \quad (20)$$

where μ represents the learning rate.

3.3. The proposed SADL method

The computational procedure of the SADL method is depicted in Fig. 2 and is elucidated as follows.

- (1) Pre-training model: Initially, the deep learning model is trained with labeled lithium-ion battery data $\{(x_i, y_i)\}_{i=1}^N$. In this stage, the deep learning model may exhibit suboptimal performance for

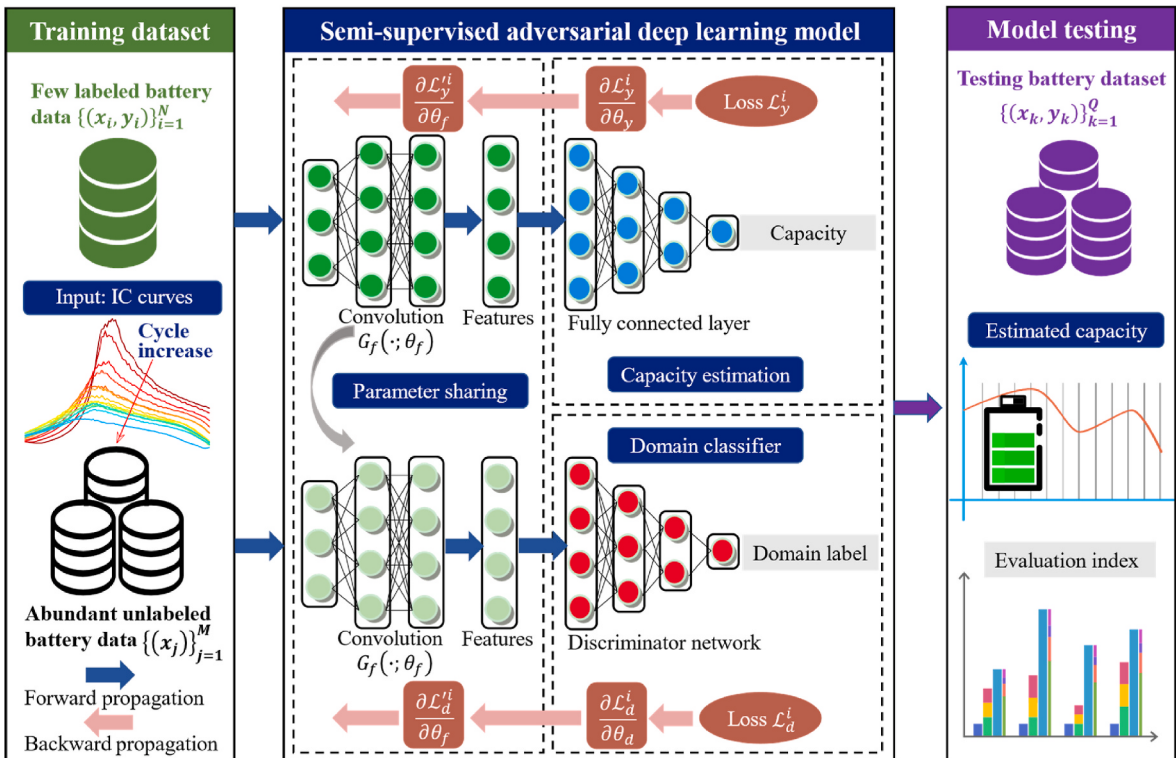


Fig. 2. Overall framework of the proposed SADL method.

- estimating battery capacity. Nevertheless, the primary objective of this phase is to establish the foundational deep learning framework, which constitutes a crucial step.
- (2) Adversarial learning: Lithium-ion battery data is partitioned into two subsets. One set comprises labeled battery training data $\{(x_i, y_i)\}_{i=1}^N$, while the other set encompasses unlabeled battery training data $\{(x_j)\}_{j=1}^M$. Adversarial training is conducted on these two lithium-ion battery datasets to enhance the overall performance of the SADL model.
 - (3) Model deployment: The SADL model is deployed in real industrial scenarios. Various types of lithium-ion batteries $\{(x_k, y_k)\}_{k=1}^Q$ are employed to assess the performance of the SADL model. A comparative analysis is conducted to evaluate and contrast the lithium-ion battery capacity estimates generated by the SADL model with those computed by other methods.

3.4. Evaluation metrics

To assess the effectiveness of capacity estimation, four evaluation metrics are employed. The absolute percentage error (APE) is utilized to identify individual errors, providing a granular perspective. Root mean squared error (RMSE) is applied for an overarching accuracy assessment. Mean absolute percentage error (MAPE) is employed to gauge the average performance. Mean deviation of MAPE (MD-MAPE) is utilized for consistency analysis. These four metrics collectively offer a comprehensive evaluation of the lithium-ion battery capacity estimation process. The specific formulas for their calculation are as follows:

$$\text{APE} = \left| \frac{\hat{y}_{i,n} - y_{i,n}}{y_{i,n}} \right| \quad (21)$$

$$\text{RMSE} = \sqrt{\frac{1}{N} \sum_{i=1}^N (\hat{y}_{i,n} - y_{i,n})^2} \quad (22)$$

$$\text{MAPE} = \frac{1}{N} \sum_{n=1}^N \left| \frac{\hat{y}_{i,n} - y_{i,n}}{y_{i,n}} \right| \quad (23)$$

$$\text{MD-MAPE} = \frac{1}{N} \sum_{n=1}^N (\text{APE}_n - \text{MAPE}) \quad (24)$$

where \hat{y} and y are the estimated capacity and actual capacity.

4. Experimental results and comparative analysis

4.1. Lithium-ion battery data set

In this work, we used the NASA randomized battery dataset and lithium-ion battery degradation dataset [53–55]. For the NASA randomized battery dataset, eight 18650 Li-ion battery cells (serial numbers: RW1, RW2, RW7, RW8, RW9, RW10, RW11, RW12) are utilized for the experimental study in this paper. The rated capacity for these batteries is 2.1 Ah. RW1, RW2, RW7, and RW8 underwent continuous operation, discharging to 3.2 V using a randomized sequence of currents (0.5 A–4 A). This method, termed random walk (RW)

discharging, involved periodic charging for randomly selected durations (0.5–3 h). After every fifty RW cycles, reference charging and discharging cycles are conducted to establish state health benchmarks. RW9, RW10, RW11, and RW12 experienced continuous operation with a sequence of charging and discharging currents (~4.5 A–4.5 A). Each loading period lasted 5 min. After 1500 periods (approximately 5 days), reference charging and discharging cycles are executed for battery state health benchmarks. The above charging and discharging parameters are shown in Table 1. For more detailed information, please refer to Refs. [53,54]. In this study, RW9, RW10, RW11, and RW12 are chosen as the training dataset. Within the training dataset, it is further divided into labeled and unlabeled subsets. The labeled subsets $\{(x_i, y_i)\}_{i=1}^N$ are RW9 and RW10. The unlabeled subsets $\{(x_j)\}_{j=1}^M$ are RW11 and RW12. The testing dataset $\{(x_k, y_k)\}_{k=1}^Q$ is RW1, RW2, RW7, and RW8.

For another NASA battery degradation dataset, B0005, B0006, B0007, B00018, B0029, B0030, B0031, and B0032 are adopted. The rated capacity for these batteries is 2 Ah. B0005, B0006, B0007, and B00018 batteries underwent three distinct operational profiles: charge, discharge, and impedance. Charging employed a constant current (CC) mode at 1.5 A until reaching 4.2 V, then transitioned to constant voltage (CV) mode until current dropped to 0.02 A. Discharge occurred at a CC of 2 A until voltage reached 2.7 V (B0005), 2.5 V (B0006), 2.2 V (B0007), and 2.5 V (B00018). For B0029, B0030, B0031, and B0032 batteries, charging employed a CC mode at 1.5 A until reaching 4.2 V, followed by CV mode until current dropped to 0.02 A. Discharge occurred at 4 A until voltage reached 2.0 V (B0029), 2.2 V (B0030), 2.5 V (B0031), and 2.7 V (B0032). The charging and discharging parameters mentioned above are presented in Table 1. Additional detailed information can be found in the literature [55]. In this work, B0029, B0030, B0031, and B0032 are selected as the training dataset. The B0029 and B0031 are considered as labeled subsets $\{(x_i, y_i)\}_{i=1}^N$, while B0030 and B0032 are treated as unlabeled subsets $\{(x_j)\}_{j=1}^M$. The testing dataset $\{(x_k, y_k)\}_{k=1}^Q$ is B0005, B0006, B0007, and B00018.

From Table 1, it can be observed that the rated capacities of the two battery datasets are 2.1 Ah and 2 Ah, respectively. To facilitate comparative calculations and analysis, the battery capacities are normalized in the subsequent computations and analyses. In this study, the labeled and unlabeled battery datasets are segregated in the training dataset. The SADL method is employed to train the model by utilizing adversarial training during the process. Specifically, adversarial training is conducted on labeled and unlabeled battery data, enhancing the feature extraction from the battery datasets. By separately investigating two distinct battery datasets, the proposed SADL method's advantage in adversarial training strategy is analysed. Additionally, the RW battery, employing various random operational conditions for charge and discharge cycles, might result in a higher battery capacity decay rate in the RW dataset.

Prior studies have compellingly established that, when compared to the direct utilization of current and voltage data from lithium-ion batteries, employing capacity increment feature curves produces superior outcomes [40,50]. This superiority stems from the heightened sensitivity of capacity increment curves, enabling a more effective capture of degradation information within the internal state of lithium-ion batteries. Such degradation information is pivotal for precisely assessing the

Table 1
Cycling parameters for different types of batteries.

Battery dataset	Battery no.	Constant current charging cutoff voltage (V)	Constant voltage charging cutoff current (A)	Constant current discharge current (A)	Constant voltage discharge cutoff voltage (V)	Battery capacity (Ah)
NASA randomized battery dataset	RW1-2	4.2	0.01	2	3.2	2.1
	RW7-12					
NASA battery degradation dataset	B0005-0007, B0018	4.2	0.02	2	2.2, 2.5, 2.7	2
	B0029-0032	4.2	0.02	4	2.0, 2.2, 2.5, 2.7	2

health and performance of the batteries. In the calculation of IC curves, the moving average method is employed for smoothing. This involved applying a windowed average to the data, effectively eliminating potential noise and fluctuations. The smoothing process enables a clearer analysis of changing trends in battery capacity, facilitating a more accurate understanding of battery performance evolution. It provides a solid foundation for further in-depth analysis by highlighting overall trends in capacity changes. The calculation results of the lithium-ion battery capacity increment curves are illustrated in Fig. 3. The x-axis represents voltage (V), and the y-axis corresponds to the capacity increment (dQ/dV).

4.2. Capacity estimation results of NASA randomized battery dataset

In the experiments of this study, to contrast with the proposed SADL method, the deep learning methods such as CNN [37–39] and LSTM [40–42] are chosen. CNN and LSTM methods are effective in estimating battery capacity by extracting features from battery data, possessing the advantage of learning complex features. Additionally, MLP, as a classic deep learning method, is selected to compare its performance with the SADL method and analyse its capabilities in battery capacity estimation. Furthermore, typical machine learning methods including AdaBoost, Decision Trees (DT), Gradient Boosting Decision Trees (GBDT), Random Forest (RF), and K-Nearest Neighbors (KNN) are also included [56]. These machine learning methods are widely applied in data mining and pattern recognition, and their performance is compared to gain insights into their respective performances in battery capacity estimation.

Deep learning methods such as CNN, LSTM, and MLP excel in learning complex feature representations from battery data but come with a higher number of model parameters and require a substantial amount of labeled data for training. On the other hand, machine learning methods often use shallow networks, have lower data requirements, but may be limited in capturing complex features. Through a comprehensive comparison of these methods, a thorough evaluation of their performance in battery capacity estimation is conducted, providing valuable information for the design of future battery management systems.

For different methods, the specific parameter designs are outlined as follows. In the SADL, the neural network is implemented as a one-dimensional CNN featuring three convolutional layers with kernel sizes of 5, 3, and 3. Max-pooling layers are applied after each convolutional layer, followed by three fully connected layers with output dimensions of 64, 32, and 1, incorporating Rectified Linear Unit activations. The neural architecture of the CNN method shares the same structure as the SADL method's neurons, but adversarial training is not employed. The MLP consists of three fully connected layers. The first layer takes an input of size 240 and outputs 63, followed by a layer

outputting 8 neurons, and a final layer producing a single-neuron output. For LSTM, the input dimension is 20 and the hidden dimension is 64. AdaBoost, DT, GBDT, RF and KNN are predominantly employed with default parameter settings. The calculation results are presented in Fig. 4.

In Fig. 4, the horizontal axis represents the number of charge-discharge cycles of the lithium-ion battery, while the vertical axis represents the normalized capacity. It is evident from Fig. 4 that the proposed SADL method closely approximates the actual measured capacity of lithium-ion batteries in its calculations. In contrast, methodologies such as CNN, MLP, LSTM, AdaBoost, DT, GBDT, RF, and KNN exhibit larger discrepancies between the calculated and actual capacities of lithium-ion batteries. The proposed SADL method achieves outstanding results, primarily by incorporating both labeled battery data $\{x_i, y_i\}_{i=1}^N$ and unlabeled battery data $\{(x_j)\}_{j=1}^M$ for model training, leading to excellent performance. In comparison, other methods like CNN, MLP, LSTM, AdaBoost, DT, GBDT, RF, and KNN rely solely on labeled battery data $\{x_i, y_i\}_{i=1}^N$ for training. When labeled data is limited, these methods exhibit poor performance, as supervised data-driven approaches heavily depend on a large dataset for effective model training. In these situations, when both labeled and unlabeled data are used for training, as seen in the proposed SADL method, it markedly enhances performance. This is the essential reason for the excellent performance of the proposed SADL method. For instance, considering the RW1 battery case, the SADL method accurately estimates the capacity in the initial stages, while other methods display notable errors. This observation suggests that the SADL method excels in the estimation of lithium-ion battery capacity. The high precision of the SADL method enables more accurate tracking of dynamic changes in battery capacity. Conversely, other methods may be more susceptible to interference, resulting in significant inaccuracies in capacity estimation. This outcome not only robustly supports the practicality of SADL in battery capacity estimation but also underscores its potential value in enhancing the accuracy of battery performance assessments. Quantitative error comparisons between the SADL method and other approaches are illustrated in Fig. 5 and Table 2.

Fig. 5 and Table 2 present the errors in estimating the capacity of lithium-ion batteries using different methods. Smaller values of error metrics indicate better performance. Clearly, the proposed SADL method demonstrates outstanding performance with an RMSE error of only 1.80%, MAPE error of 1.83%, and MD-MAPE error of 1.05%. In contrast, other methods such as CNN, MLP, LSTM, AdaBoost, DT, GBDT, RF, and KNN exhibit higher RMSE, MAPE, and MD-MAPE, indicating larger errors in their estimation processes. Among them, methods with shallow network structures like AdaBoost show significant errors, with RF having the largest errors, reaching 5.79%, 7.08%, and 3.28% for RMSE, MAPE, and MD-MAPE, respectively. Additionally, the APE

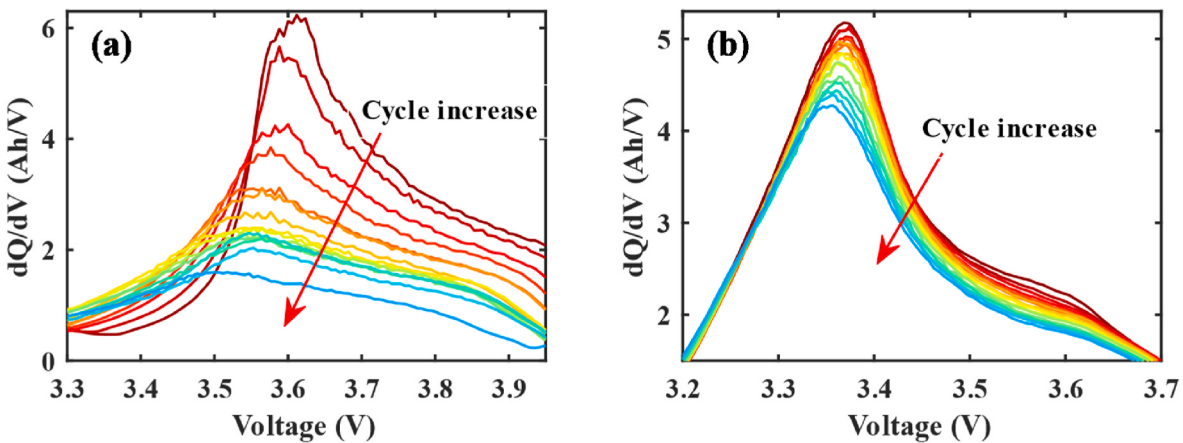


Fig. 3. The IC curves of different batteries. (a) RW9; (b) B0029.

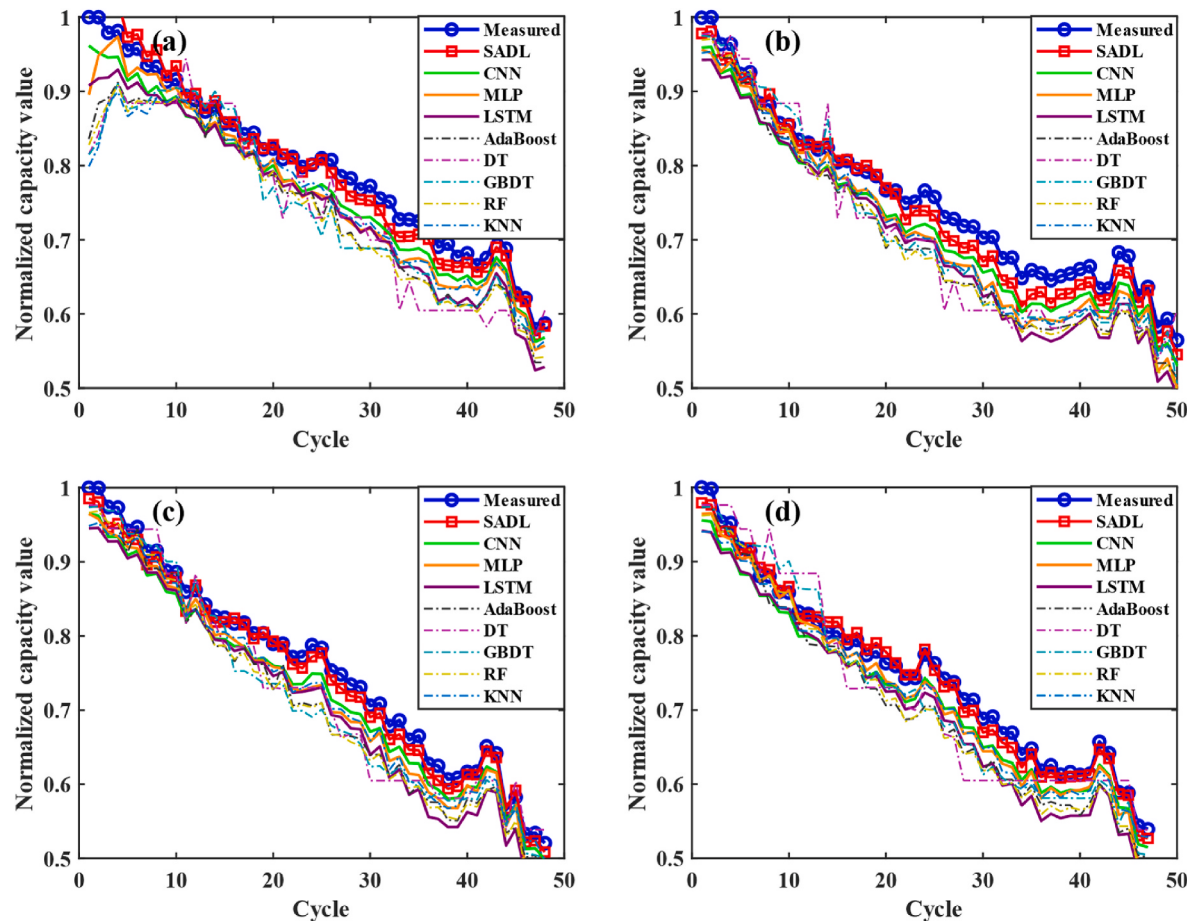


Fig. 4. Capacity estimation of NASA randomized battery dataset. (a) RW1; (b) RW2; (c) RW7; (d) RW8.

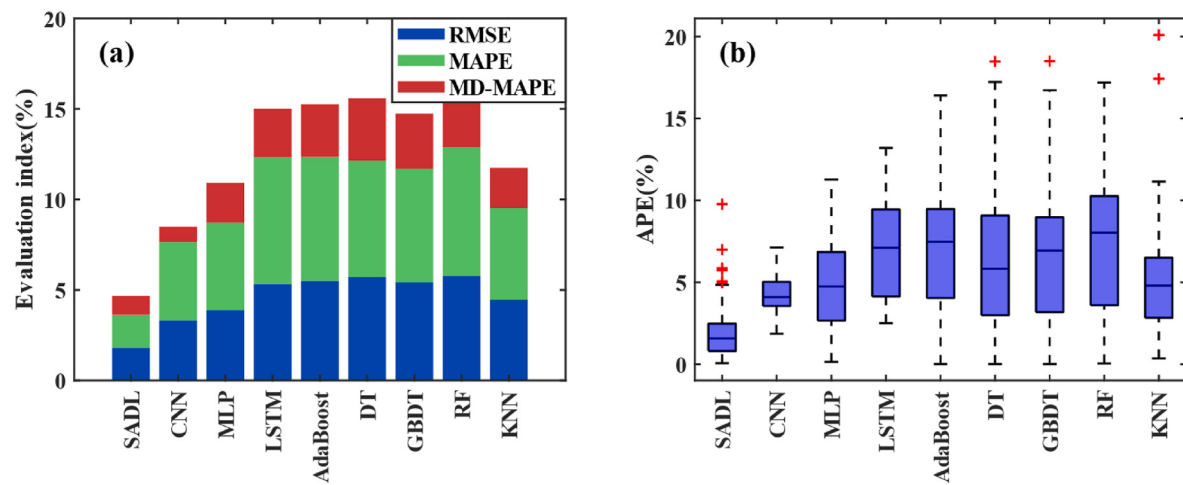


Fig. 5. Evaluation index of NASA randomized battery dataset. (a) RMSE, MAPE, MD-MAPE; (b) APE.

boxplot error shown in Fig. 5(b) visually confirms that SADL has the smallest error, followed by CNN, MLP, and LSTM methods, while RF exhibits the largest error. This is primarily because SADL enhances model performance through semi-supervised training using both labeled and unlabeled battery data. Experimental results indicate that the proposed SADL method is effective and capable of accurately estimating the capacity of lithium-ion batteries. In summary, the superior performance of the SADL method across these evaluation metrics provides robust support for its reliability and accuracy in estimating lithium-ion battery

capacity.

4.3. Capacity estimation results of NASA battery degradation dataset

The comparative analysis contrasts the outcomes derived from the SADL method with those generated by CNN, MLP, LSTM, AdaBoost, DT, GBDT, RF, and KNN in the estimation of lithium-ion battery capacity. The results are illustrated in Fig. 6.

The horizontal and vertical axes in Fig. 6 represent the number of

Table 2
Evaluation results of NASA randomized battery dataset.

Methods	RMSE (%)	MAPE (%)	MD-MAPE (%)
SADL (proposed)	1.80	1.83	1.05
CNN	3.32	4.32	0.85
MLP	3.89	4.83	2.20
LSTM	5.33	7.00	2.68
AdaBoost	5.51	6.83	2.91
DT	5.73	6.42	3.44
GBDT	5.42	6.27	3.05
RF	5.79	7.08	3.28
KNN	4.46	5.07	2.22

charge-discharge cycles of the battery and the normalized capacity value, respectively. It is evident from Fig. 6 that the estimated lithium-ion battery capacity using the SADL method closely aligns with the actual measured capacity. In contrast to methods such as CNN, MLP, and LSTM, the SADL method exhibits superior performance with smaller errors. When compared to shallow neural networks like AdaBoost, DT, GBDT, RF, and KNN, the SADL method stands out with exceptional performance. It is particularly noteworthy that, in the initial and final stages of lithium-ion battery capacity estimation, the performance of shallow neural networks such as AdaBoost, DT, GBDT, RF, and KNN is comparatively poor. The effectiveness of the SADL method is attributed to the simultaneous utilization of labeled and unlabeled battery data during model training, enhancing model performance by leveraging unlabeled data. Conversely, methods like CNN, MLP, LSTM, AdaBoost, DT, GBDT, RF, and KNN rely on a limited amount of labeled data for model training, making it challenging to achieve optimal performance due to the scarcity of data. Therefore, in scenarios with limited labeled data, the SADL method significantly improves training results by

incorporating unlabeled data. The quantitative error comparison between the SADL method and other approaches is illustrated in Fig. 7 and Table 3.

Fig. 7 and Table 3 present the errors of different methods, where larger errors indicate poorer performance. Clearly, the proposed SADL method demonstrates the smallest errors, with RMSE, MAPE, and MD-MAPE reaching only 2.55%, 2.53%, and 1.72%, respectively. In contrast, CNN, MLP, LSTM, AdaBoost, DT, GBDT, RF, and KNN exhibit larger errors, with KNN showing the maximum errors, reaching 12.48%, 12.97%, and 10.30% for RMSE, MAPE, and MD-MAPE, respectively. Deep learning methods such as CNN, MLP, and LSTM show less favorable results in terms of RMSE, MAPE, and MD-MAPE, while machine learning methods like AdaBoost, DT, GBDT, RF, and KNN demonstrate larger errors. From the APE boxplot results in Fig. 7(b), the proposed SADL method has the smallest error, followed by CNN. In contrast, AdaBoost, DT, GBDT, RF, and KNN exhibit larger APE errors, indicating the superior performance of SADL. The superior performance of the proposed SADL method is fundamentally attributed to the comprehensive utilization of both labeled and unlabeled battery data during model training, enhancing the overall performance of the model. Deep learning methods like CNN, MLP, and LSTM struggle to train the model with a limited amount of labeled battery data, while machine learning methods like AdaBoost, DT, GBDT, RF, and KNN show even poorer results with limited labeled battery data. The experimental results indicate that simultaneously leveraging labeled and unlabeled battery data for model training significantly improves training outcomes. Therefore, SADL emerges as a standout performer in the capacity estimation task, providing substantial support for its extensive application in the field of lithium-ion battery performance assessment.

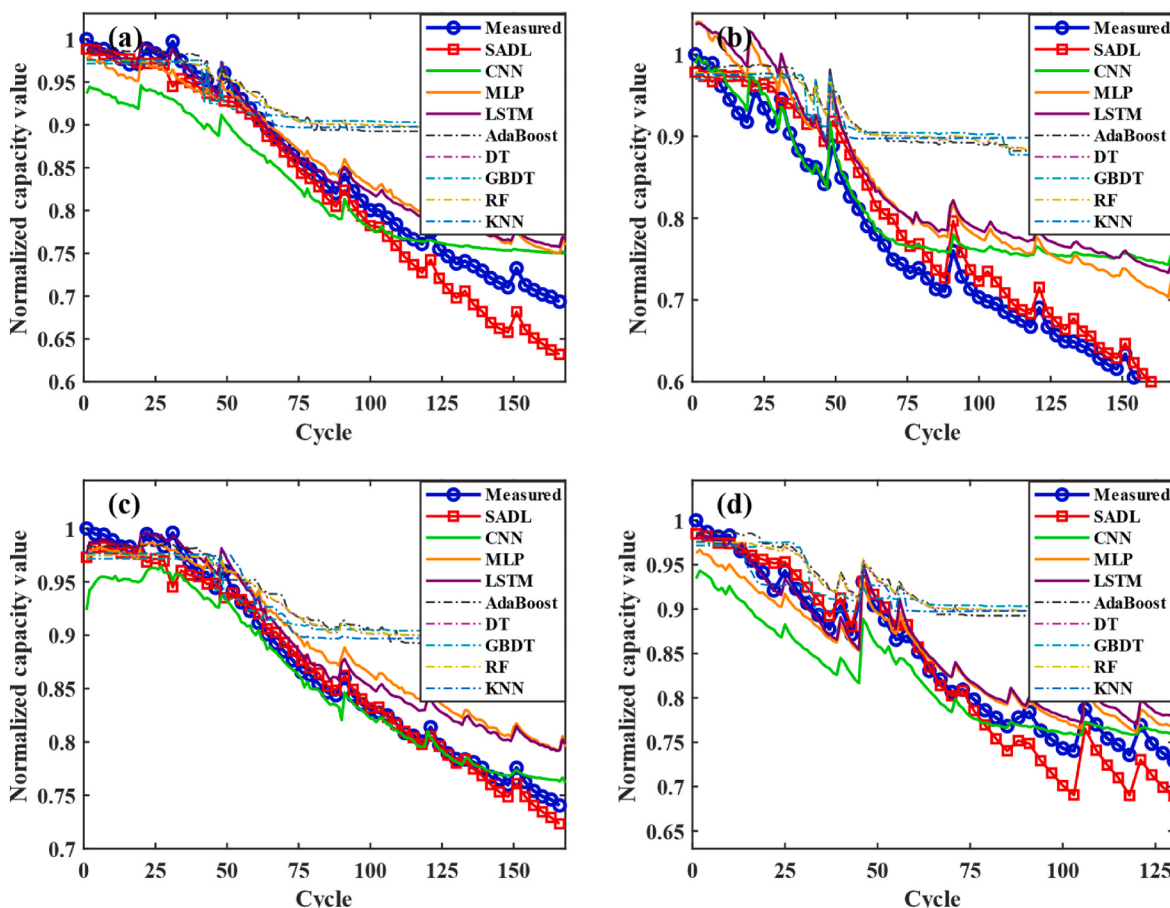


Fig. 6. Capacity estimation of NASA battery degradation dataset. (a) B0005; (b) B0006; (c) B0007; (d) B0018.

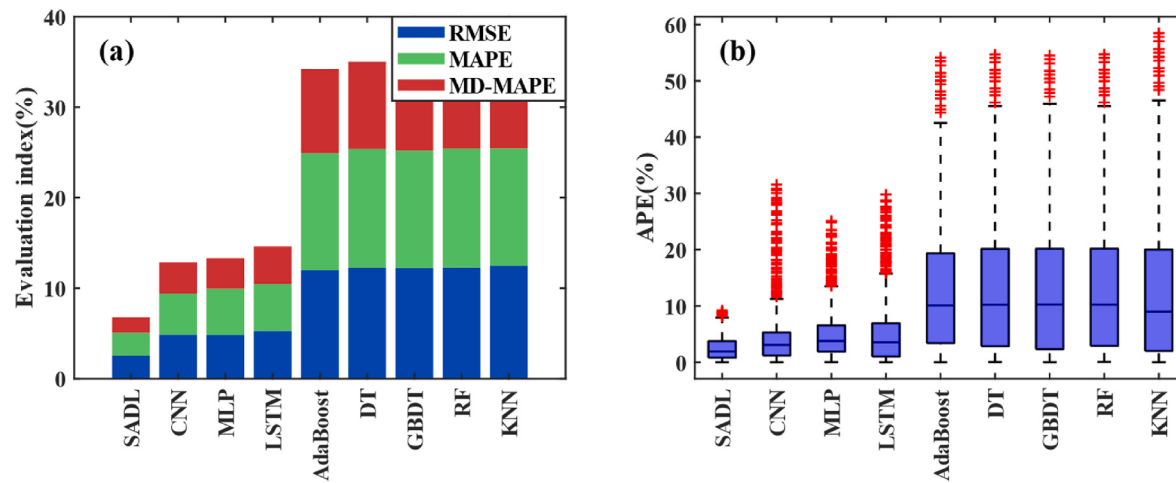


Fig. 7. Evaluation index of NASA battery degradation dataset. (a) RMSE, MAPE, MD-MAPE; (b) APE.

Table 3
Evaluation results of NASA battery degradation dataset.

Methods	RMSE (%)	MAPE (%)	MD-MAPE (%)
SADL (proposed)	2.55	2.53	1.72
CNN	4.86	4.56	3.42
MLP	4.82	5.13	3.36
LSTM	5.28	5.20	4.14
AdaBoost	12.01	12.92	9.29
DT	12.25	13.13	9.63
GBDT	12.19	13.01	9.69
RF	12.27	13.16	9.63
KNN	12.48	12.97	10.30

5. Conclusions

Accurately estimating the capacity of lithium-ion batteries is essential for developing effective energy utilization strategies and addressing safety concerns in BESS. In scenarios involving battery usage, such as grid energy storage and electric vehicles, the availability of labeled data for voltage, current, and capacity is often limited, with the majority of data being unlabeled. Acquiring capacity labels necessitates complete charge and discharge cycles, making it challenging to obtain labeled data. Limited labeled data poses challenges in training accurate and reliable deep learning models. Therefore, a SADL method is proposed to enhance the accuracy of battery capacity estimation by effectively utilizing both labeled and unlabeled battery data.

Experimental results demonstrate that the proposed SADL method significantly improves battery capacity estimation, achieving RMSE, MAPE, and MD-MAPE errors of approximately 2%. This represents a substantial advancement in accurate battery capacity estimation. In contrast, other methods such as CNN, MLP, LSTM, AdaBoost, DT, GBDT, RF, and KNN exhibit larger errors, some exceeding 10%. This highlights the substantial performance improvement achieved by the SADL method through the simultaneous utilization of labeled and unlabeled battery data in capacity estimation.

Appendix

See Table A.1.

However, the SADL method has certain limitations, such as not incorporating knowledge from the physical-chemical models of batteries. In the future, integrating the operational mechanisms of specific batteries into the model holds the potential to further enhance the reliability and accuracy of the model.

CRediT authorship contribution statement

Jiachi Yao: Writing – original draft, Software, Methodology, Investigation, Conceptualization. **Zhonghao Chang:** Writing – review & editing, Visualization, Investigation. **Te Han:** Writing – review & editing, Supervision, Methodology, Funding acquisition, Conceptualization. **Jingpeng Tian:** Writing – review & editing, Supervision, Investigation, Funding acquisition.

Declaration of competing interest

The authors declare that they have no known competing financial interests or personal relationships that could have appeared to influence the work reported in this paper.

Data availability

Data will be made available on request.

Acknowledgements

This work was supported by the National Natural Science Foundation of China (Grant Nos. 72201152 and 52207229), the Young Elite Scientists Sponsorship Program by CAST (Grant No. 2023QNRC001), the Anhui Provincial Science and Technology Major Project (Grant No. 2023z020006), the Beijing Association for Science and Technology Youth Talent Lifting Project, the Young Teachers' Scientific Research Ability Improvement Program of Beijing University of Civil Engineering and Architecture (No.X23004).

Table A.1
Abbreviation of terms.

Abbreviation	Explanation	Abbreviation	Explanation
BESS	Battery energy storage systems	ECM	Equivalent Circuit Model
RC	Resistor-Capacitor	SADL	Semi-supervised Adversarial Deep Learning
IC	Incremental Capacity	CNN	Convolutional Neural Network
LSTM	Long Short-Term Memory	MLP	Multi-Layer Perceptron
GAN	Generative Adversarial Network	SVM	Support Vector Machine
DT	Decision Tree	GBDT	Gradient Boosting Decision Tree
RF	Random Forest	KNN	K-Nearest Neighbors
APE	Absolute Percentage Error	RMSE	Root Mean Squared Error
MAPE	Mean Absolute Percentage error	MD-MAPE	Mean Deviation of MAPE

References

- [1] Han T, Tian JP, Chung CY, et al. Challenges and opportunities for battery health estimation: bridging laboratory research and real-world applications. *J Energy Chem* 2024;89:434–6.
- [2] Qiu XH, Wang SF, Chen K. A conditional generative adversarial network-based synthetic data augmentation technique for battery state-of-charge estimation. *Appl Soft Comput* 2023;142:110281.
- [3] Gao RB, Tao JL, Zhang JY, et al. NSGA-III-SD based Fuzzy energy management system optimization for lithium battery/supercapacitor HEV. *Appl Soft Comput* 2023;142:110280.
- [4] Tian JP, Xiong R, Shen WX, et al. Deep neural network battery charging curve prediction using 30 points collected in 10 min. *Joule* 2021;5(6):1521–34.
- [5] Ren D, Hsu H, Li R, et al. A comparative investigation of aging effects on thermal runaway behavior of lithium-ion batteries. *ETransportation* 2019;2:100034.
- [6] Tang AH, Wu ZK, Xu TT, et al. Week-level early warning strategy for thermal runaway risk based on real-scenario operating data of electric vehicles. *ETransportation* 2024;19:100308.
- [7] Tian JP, Xiong R, Shen WX, et al. Electrode ageing estimation and open circuit voltage reconstruction for lithium ion batteries. *Energy Storage Mater* 2021;37:283–95.
- [8] Li JW, He SC, Yang QQ, et al. A comprehensive review of second life batteries toward sustainable mechanisms: potential, challenges, and future prospects. *IEEE T Transp Electr* 2023;9(4):4824–45.
- [9] Meng HX, Geng MY, Xing JD, et al. A hybrid method for prognostics of lithium-ion batteries capacity considering regeneration phenomena. *Energy* 2022;261:125278.
- [10] Narayanan SSS, Thangavel S. Terminal voltage prediction of Li-ion batteries using combined neural network and teaching learning based optimization algorithm. *Appl Soft Comput* 2023;133:109954.
- [11] Ghosh N, Garg A, Panigrahi BK, et al. An evolving quantum fuzzy neural network for online state-of-health estimation of Li-ion cell. *Appl Soft Comput* 2023;143:110263.
- [12] Ding SC, Li YD, Dai HF, et al. Accurate model parameter identification to boost precise ageing prediction of lithium-ion batteries: a review. *Adv Energy Mater* 2023;51:158201.
- [13] Chen ZW, Zhang SY, Shi N, et al. Online state-of-health estimation of lithium-ion battery based on relevance vector machine with dynamic integration. *Appl Soft Comput* 2022;129:109615.
- [14] Ates M, Chebil A. Supercapacitor and battery performances of multi-component nanocomposites: real circuit and equivalent circuit model analysis. *J Energy Storage* 2022;53:105093.
- [15] Hariharan KS. A coupled nonlinear equivalent circuit – thermal model for lithium ion cells. *J Power Sources* 2013;227:171–6.
- [16] Farmann A, Sauer DU. Comparative study of reduced order equivalent circuit models for on-board state-of-available-power prediction of lithium-ion batteries in electric vehicles. *Appl Energy* 2018;225:1102–22.
- [17] Yang JF, Cai YF, Pan CF, et al. A novel resistor-inductor network-based equivalent circuit model of lithium-ion batteries under constant-voltage charging condition. *Appl Energy* 2019;254:113726.
- [18] Yang JF, Huang WX, Xia B, et al. The improved open-circuit voltage characterization test using active polarization voltage reduction method. *Appl Energy* 2019;237:682–94.
- [19] Hosseiniinasab S, Lin CW, Pischinger S, et al. State-of-health estimation of lithium-ion batteries for electrified vehicles using a reduced-order electrochemical model. *J Energy Storage* 2022;52:104684.
- [20] Hahn Y, Gao ZY, Nguyen TT, et al. A reduced order model for a lithium-ion 3D pouch battery for coupled thermal-electrochemical analysis. *J Energy Storage* 2023;70:107966.
- [21] Hu XS, Li SB, Peng H. A comparative study of equivalent circuit models for Li-ion batteries. *J Power Sources* 2012;198:359–67.
- [22] Peng JC, Meng JH, Wu J, et al. A comprehensive overview and comparison of parameter benchmark methods for lithium-ion battery application. *J Energy Storage* 2023;71:108197.
- [23] Doyle M, Fuller TF, Newman J. Modeling of Galvanostatic charge and discharge of the lithium/polymer/insertion cell. *J Electrochem Soc* 1993;140(6):1526–33.
- [24] Fuller TF, Doyle M, Newman J. Simulation and optimization of the dual lithium ion insertion cell. *J Electrochem Soc* 1994;141(1):1–10.
- [25] Jokar A, Rajabloo B, Désilets M, et al. Review of simplified pseudo-two-dimensional models of lithium-ion batteries. *J Power Sources* 2016;327:44–55.
- [26] Lin XW, Zhou ZF, Zhu XG, et al. Non-uniform thermal characteristics investigation of three-dimensional electrochemical-thermal coupled model for pouch lithium-ion battery. *J Clean Prod* 2023;417:137912.
- [27] Petit M, Calas E, Bernard J. A simplified electrochemical model for modelling Li-ion batteries comprising blend and bidispersed electrodes for high power applications. *J Power Sources* 2020;479:228766.
- [28] Mehta R, Gupta A. An improved single-particle model with electrolyte dynamics for high current applications of lithium-ion cells. *Electrochim Acta* 2021;389:138623.
- [29] Torchio M, Magni L, Gopaluni RB, et al. LIONSIMBA: a matlab framework based on a finite volume model suitable for Li-ion battery design, simulation, and control. *J Electrochem Soc* 2016;163(7):1192–205.
- [30] Xiong R, Li LL, Li ZR, et al. An electrochemical model based degradation state identification method of Lithium-ion battery for all-climate electric vehicles application. *Appl Energy* 2018;129:264–75.
- [31] Zhu XF, Wang W, Zou GP, et al. State of health estimation of lithium-ion battery by removing model redundancy through aging mechanism. *J Energy Storage* 2022;52:105018.
- [32] Naseri F, Schatzl E, Stroe DI, et al. An enhanced equivalent circuit model with real-time parameter identification for battery state-of-charge estimation. *IEEE Trans Ind Electron* 2022;69(4):3743–51.
- [33] Miguel E, Plett GL, Trimboli MS, et al. Review of computational parameter estimation methods for electrochemical models. *J Energy Storage* 2021;44:103388.
- [34] Xue AR, Yang WL, Yuan XM, et al. Estimating state of health of lithium-ion batteries based on generalized regression neural network and quantum genetic algorithm. *Appl Soft Comput* 2022;130:109688.
- [35] Wu MY, Zhong YM, Wu J, et al. State of health estimation of the lithium-ion power battery based on the principal component analysis-particle swarm optimization-back propagation neural network. *Energy* 2023;581:129061.
- [36] Sun T, Wu RJ, Cui YF, et al. Sequent extended Kalman filter capacity estimation method for lithium-ion batteries based on discrete battery aging model and support vector machine. *J Energy Storage* 2023;39:102594.
- [37] Xu HW, Wu LF, Xiong SZ, et al. An improved CNN-LSTM model-based state-of-health estimation approach for lithium-ion batteries. *Energy* 2023;276:127585.
- [38] Chen SZ, Liang ZK, Yuan HL, et al. A novel state of health estimation method for lithium-ion batteries based on constant-voltage charging partial data and convolutional neural network. *Energy* 2023;283:129103.
- [39] Tang AH, Jiang YH, Yu QQ, et al. A hybrid neural network model with attention mechanism for state of health estimation of lithium-ion batteries. *J Energy Storage* 2023;68:107734.
- [40] Meng HX, Geng MY, Han T. Long short-term memory network with Bayesian optimization for health prognostics of lithium-ion batteries based on partial incremental capacity analysis. *Reliab Eng Syst Saf* 2023;236:109288.
- [41] Wang SL, Takvi AP, Jin SY, et al. An improved sliding window-long short-term memory modeling method for real-world capacity estimation of lithium-ion batteries considering strong random charging characteristics. *J Energy Storage* 2023;70:108038.
- [42] El DM, Al GM, El MA, et al. Capacity estimation of lithium-ion batteries based on adaptive empirical wavelet transform and long short-term memory neural network. *J Energy Storage* 2023;70:108046.
- [43] Cao MD, Zhang T, Wang J, et al. A deep belief network approach to remaining capacity estimation for lithium-ion batteries based on charging process features. *J Energy Storage* 2022;48:103825.
- [44] Wang Z, Yang FF, Xu Q, et al. Capacity estimation of lithium-ion batteries based on data aggregation and feature fusion via graph neural network. *Appl Energy* 2023;336:120808.
- [45] Tang AH, Huang YK, Xu YC, et al. Data-physics-driven estimation of battery state of charge and capacity. *Energy* 2024;294:130776.
- [46] Xiong R, Tian JP, Shen WX, et al. Semi-supervised estimation of capacity degradation for lithium ion batteries with electrochemical impedance spectroscopy. *J Energy Chem* 2023;76:404–13.

- [47] Salucci CB, Bakdi A, Glad IK, et al. A novel semi-supervised learning approach for State of Health monitoring of maritime lithium-ion batteries. *J Power Sources* 2023;556:232429.
- [48] Wu J, Cui XC, Meng JH, et al. Data-driven transfer-stacking-based state of health estimation for lithium-ion batteries. *IEEE Trans Ind Electron* 2024;71(1):604–14.
- [49] Han T, Wang Z, Meng HX. End-to-end capacity estimation of Lithium-ion batteries with an enhanced long short-term memory network considering domain adaptation. *J Power Sources* 2022;520:230823.
- [50] Yao JC, Han T. Data-driven lithium-ion batteries capacity estimation based on deep transfer learning using partial segment of charging/discharging data. *Energy* 2023;271:127033.
- [51] Huang K, Yao KX, Guo YF, et al. State of health estimation of lithium-ion batteries based on fine-tuning or rebuilding transfer learning strategies combined with new features mining. *Energy* 2023;282:128739.
- [52] Goodfellow IJ, Pouget-Abadie J, Mirza M, et al. Generative adversarial nets[C]. NIPS; 2014.
- [53] Bole B, Kulkarni CS, Daigle M. Adaptation of an electrochemistry-based Li-Ion battery model to account for deterioration observed under randomized use. In: Conference of the prognostics & health management society; 2014.
- [54] B. Bole, C. Kulkarni, and M. Daigle. Randomized Battery Usage Data Set. NASA Ames Prognostics Data Repository (<http://ti.arc.nasa.gov/project/prognostic-data-repository>), NASA Ames Research Center, Moffett Field, CA.
- [55] Saha B, Goebel K. Battery data set. NASA AMES Prognostics Data Repository; 2007.
- [56] Huang ZJ, Sugiarto L, Lu YC. Feature-target pairing in machine learning for battery health diagnosis and prognosis: a critical review. *ECOMAT* 2023;5(6):e12345.